International Journal of Pharmaceutics 696 (2026) 126825

Contents lists available at ScienceDirect

International Journal of Pharmaceutics

journal homepage: www.elsevier.com/locate/ijpharm

Process-guided design of nanoliposomal vitamin D3: formulation, stability and quality by design mapping

Diego Caccavo [a,b], Luca Broegg [b], Gaetano Lamberti [a,b,*], Raffaella De Piano [a], Anna Angela Barba [b,c]

[a] Dipartimento di Ingegneria Industriale, Università degli Studi di Salerno, Via Giovanni Paolo II, 132, 84084 Fisciano, SA, Italy
[b] Enhanced Systems and Technologies Srl, Via Circumvallazione 39, 83100 Avellino, Italy
[c] Dipartimento di Farmacia, Università degli Studi di Salerno, Via Giovanni Paolo II, 132, 84084 Fisciano, SA, Italy

ARTICLE INFO

Keywords:
Vitamin D_3
Nanoliposomes
Coaxial-jet mixing
Box–Behnken design
Quality-by-Design

ABSTRACT

The development of aqueous vitamin D_3 supplements remains challenging because the molecule is poorly soluble, chemically fragile, and prone to loss of potency during storage. In this work, we adopted a Quality-by-Design (QbD) strategy to construct a nanoliposomal structure able to protect and deliver vitamin D_3 while maintaining technological simplicity and high tolerability. As a first step, drug-free nanoliposomes were produced using a coaxial-jet mixer and systematically investigated through a Box–Behnken Design. This approach allowed us to identify the critical relationships between phosphatidylcholine concentration, solvent/antisolvent flow rates, and the resulting nanoliposomal architecture, thereby defining a robust design space for nano-vesicle formation. Vitamin D_3 was then introduced into the optimized system to verify process transferability. Encapsulation proved efficient and compatible with the micromixing-driven assembly of nanoliposomes, and the formulation was subsequently subjected to accelerated and real-time stability studies. These experiments revealed a clear hierarchy of stabilizing effects, highlighting the combined protective role of the liposomal bilayer and a carefully balanced antioxidant environment. Building on these findings, the research formulation was further refined into a commercially viable product, described in a dedicated patent, and benchmarked against leading marketed references. The final dispersion exhibited high structural uniformity, stable vitamin retention and manufacturing features consistent with large-scale implementation. Overall, this work demonstrates how a QbD-guided pathway — from mechanistic process mapping to stability-driven optimization and product translation — can yield a high-quality nanoliposomal vitamin D_3 with clear technological and practical advantages.

1. Introduction

Vitamin D_3 (cholecalciferol) is essential for calcium–phosphate homeostasis and musculoskeletal health, with mounting evidence for broader roles in immune and cardiometabolic function. Yet its deficiency remains widespread in Europe and beyond: standardized surveys report concerning prevalence requiring public-health action, with many subgroups far below sufficiency cut-offs (e.g., <50 nmol/L (Cashman et al., 2016).

Clinically, vitamin D_3 is generally favored over vitamin D_2 for raising and maintaining serum 25(OH)D, as shown by a large meta-analysis (Tripkovic et al., 2012).

Dosing pattern also matters. Several analyses suggest that smaller daily doses achieve more consistent physiology than intermittent boluses, which can be ineffective or even counterproductive for extra-skeletal outcomes (Adami and Fassio, 2021; Mazess et al., 2021).

Despite its clinical importance, oral delivery of vitamin D_3 remains a formulation challenge. As a highly lipophilic molecule, D_3 is commonly dosed in oils or solid dosage forms that can be poorly palatable, slow to absorb, or unstable in aqueous settings. Stability studies show rapid degradation of D_3 in water under light/oxygen and at unfavorable pH or ionic strengths (Temova Rakuša et al., 2021).

Lipid-based systems (including emulsions, self-emulsifying systems, and liposomes) are established strategies to improve oral exposure of hydrophobic actives by promoting solubilization and intestinal processing into mixed micelles (Pouton and Porter, 2008).

* Corresponding author at: Dipartimento di Ingegneria Industriale, Università degli Studi di Salerno, Via Giovanni Paolo II, 132, 84084 Fisciano, SA, Italy.
E-mail address: glamberti@unisa.it (G. Lamberti).

https://doi.org/10.1016/j.ijpharm.2026.126825
Received 5 February 2026; Received in revised form 8 March 2026; Accepted 27 March 2026
Available online 29 March 2026

Vitamins have been successfully encapsulated in liposomes, among other ways (Bondu and Yen, 2022; Chaves et al., 2023b; Sameer Khan et al., 2024), using ultrasonic energy (Bochicchio et al., 2016), in which vitamins E, D_2, and B_{12} were tested, and using a patented coaxial system known as simil-microfluidic technology (Barba et al., 2017; Bochicchio et al., 2017; Bochicchio et al., 2020a; Bochicchio et al., 2020b; Bochicchio et al., 2017; Dalmoro et al., 2019). This technology, in particular, was found to be particularly effective working with lipophilic molecules, such as vitamins D_3 and K_2.

For vitamin D_3 specifically, recent studies indicate that nanoscale liposomal carriers are of great interest (Amjadi et al., 2024; Chaves et al., 2023a; Fan et al., 2023; Rudzińska et al., 2024) and they can elevate serum 25(OH)D more effectively than oil solutions, with faster early absorption and higher exposure (Dałek et al., 2022; Żurek et al., 2023).

However, many aqueous "liposomal" products on the market remain micrometric and polydisperse, often relying on high levels of salts, co-solvents, viscosity modifiers, or surfactants to stave off coalescence and oxidative loss – approaches traceable to early stabilization patents for aqueous vitamin D (e.g., combinations of nonionic surfactants with chelators/antioxidants) (Makino et al., 1993).

From a process-engineering standpoint, the particle-size distribution (PSD) of liposomes formed by antisolvent mixing is governed by micromixing kinetics, as clarified in microfluidic approaches (Akar et al., 2024; Lim et al., 2020; Mehraji and DeVoe, 2024; Pittiu et al., 2024). Coaxial turbulent-jet mixers can achieve ultra-fast mixing and high throughput, enabling narrower PSDs and scalable manufacturing – principles established in the flash nanoprecipitation literature and demonstrated for lipid nanoparticles (Caccavo et al., 2023; Lim et al., 2014; Saad and Prud'homme, 2016).

The global nutraceutical sector is experiencing sustained growth due to rising preventive-health awareness, ageing populations and the shift from treatment to wellness consumption. For example, the global market was valued at approximately USD 591.1 billion in 2024 and is projected to reach about USD 919.1 billion by 2030, corresponding to a Compound Annual Growth Rate (CAGR) of ~7.6 % between 2025 and 2030 (Grand View Research, 2024b). Within that broad context, the dietary supplements market specifically is forecast to grow from some USD 192.7 billion in 2024 to about USD 414.5 billion by 2033 (CAGR ~8.9 %) (Grand View Research, 2024a). Focusing more narrowly on vitamin D and vitamin D_3, a recent study estimates that the global vitamin D market (including food-fortification, feed, supplements, etc.) was about USD 1.23 billion in 2021, with a projected reach of USD 2.40 billion by 2030 (CAGR ~7.6 %) (Spherical Insights, 2024). Another report specific to vitamin D_3 forecasts a CAGR of ~4.5 % from 2025 to 2034, with the market reaching ~USD 524.1 million by 2034 from ~USD 337.5 million in 2024 (Market.us, 2025). Moreover, the vitamin D supplements sub-market (which is directly relevant to our work) is estimated at about USD 5.22 billion in 2025, rising to USD 7.96 billion by 2030 (CAGR ~8.79 %) (Mordor Intelligence, 2025). Taken together, these market figures reflect a strong and growing opportunity for advanced, high-quality vitamin D_3 formulations, particularly those that address key aspects such as bioavailability, palatability and stability – areas where existing products often under-perform.

While both Quality-by-Design approaches (Buttitta et al., 2024; Penoy et al., 2024) and coaxial mixing technologies have been previously applied to nanoparticle and liposome production, their combined use to systematically elucidate the relationships between hydrodynamic conditions, vesicle formation, and formulation stability in vitamin D3 systems has received limited attention (Guimarães et al., 2021; Sainaga Jyothi et al., 2022). In this work, the coaxial-jet mixer is used not merely as a production device but as a controllable platform to investigate how micromixing intensity and formulation parameters influence the nanoscale architecture of liposomes. By integrating response-surface modeling, process hydrodynamics, and stability analysis within a unified framework, the present study aims to clarify the process–structure relationships underlying the formation of stable nanoliposomal vitamin D3 systems.

Building on these clinical and engineering drivers, we sought to develop an additive-lean, aqueous, nanoliposomal vitamin D_3 that is physically stable, palatable (water-like viscosity), and industrially scalable. Our approach integrates (i) a coaxial-jet nanoprecipitation process to control nucleation/growth and PSD, and (ii) a minimalistic composition that leverages phosphatidylcholine bilayers and a restrained antioxidant/buffer system to mitigate oxidation and isomerization without resorting to high salt or gelling loads. The formulation concept – composition ranges, stabilizing roles of α-tocopherol and citric/citrate/ascorbate, and avoidance of viscosity enhancers – together with the process window allow us to obtain a fully compliant nanoliposomal solution.

Unlike previous studies on coaxial-jet mixers, which mainly focused on hydrodynamic characterization, the present work integrates process mapping with formulation performance, explicitly linking mixing conditions to liposome architecture, stability and practical usability.

2. Materials and methods

2.1. Materials

Soy lecithin PWD E322 (CAS 8002-43-5) was purchased from A.C.E. F. S.r.L. (Piacenza, Italy). Vitamin D_3 (cholecalciferol, ≥97 %, CAS 67-97-0) and Vitamin E (alpha-tocopherol, ≥96 %, CAS 10191-41-0) were obtained from Sigma-Aldrich (Milan, Italy). Ethanol >99.5 % vol (CAS 64-17-5), citric acid E330 (CAS 77-92-9), trisodium citrate dihydrate E311 (CAS 6132-04-3), sodium ascorbate E301 (CAS 134-03-2), potassium sorbate E202 (CAS 24634-61-5) and sodium benzoate E211 (CAS 532-32-1), were purchased from A.C.E.F. SrL (Piacenza, Italy),

The lecithin powder has been purified as follows: it was mixed in pure ethanol at a 1:1.5 ratio, and the suspension was stirred on a rotating plate for at least 15 h. The suspension was centrifuged (10 min at 6500 rpm) using a centrifuge (NEYA 16 HIGH SPEED, Giorgio Bormac S.r.L, Modena, Italia), and the supernatant was recovered, consisting of ethanol-lecithin solution with a higher percentage of phosphatidylcholine. More details can be found in Caccavo et al. (2025).

For the aqueous phase deionized water was used, all other reagents were analytical grade and used as received.

2.2. Methods

2.2.1. Liposome production by coaxial-jet mixing

Nanoliposomes were produced using a custom-built coaxial-jet turbulent mixer (CJTM) (Caccavo et al., 2023), following the simil-microfluidic approach introduced formerly (Barba et al., 2017). The CJTM was constructed from commercially available components to ensure reproducibility and ease of assembly. The mixer head comprised a vertical coaxial injection system consisting of a 23 G BD Quincke spinal needle (90 mm length) inserted into a PVC pipe with 3 mm internal diameter, forming the inner and outer fluid conduits, respectively. This assembly was mounted on an aluminium support (Combitech® aluminium square-tube system) to maintain stable vertical alignment essential for consistent coaxial flow. The organic solvent (lipid solution) was delivered through the spinal needle using a Sono-Tek 12-05126 dual syringe pump, while the aqueous antisolvent was supplied via a continuous push–pull syringe pump to achieve pulsation-free, high flow rates (Iannone et al., 2022). All fluid connections were secured with standard PVC tubing and Luer-lock fittings to minimize dead volume and prevent leakage during operation (Caccavo et al., 2023).

The solvent stream (inner line) contained the lipid solution with or without vitamin D_3 and antioxidants. The antisolvent stream (outer line) consisted of deionized water containing, for different formulations, sodium ascorbate, potassium sorbate, sodium benzoate and a citric acid/sodium citrate buffer (pH 4.5–5.5). During operation, the two streams formed a coaxial jet. Rapid solvent exchange induced supersaturation

and spontaneous phospholipid self-assembly into nanoscale liposomes. For vitamin D_3-loaded liposomes, the feed ratio was 10 % w/w of PC. The resulting dispersion was diluted with the same buffer, yielding 50 μg mL^{-1} (2000 IU mL^{-1}) in the final product.

Within such a configuration, the mixer's performance is governed by two dimensionless parameters: the mixture Reynolds number ($N_{Re_{mix}}$), which captures the relative influence of inertial to viscous forces, and the Flow Momentum Ratio (*FMR*), which expresses the relative momentum between the solvent and antisolvent streams. High $N_{Re_{mix}}$ and appropriately balanced *FMR* promote the formation of a turbulent jet at the outlet of the internal conduit. Under these conditions, eddies and vortical structures rapidly stretch and fold the fluid interface, leading to mixing times orders of magnitude shorter than in laminar or diffusion-limited regimes.

The rapid and intense micromixing achieved in the turbulent regime drives homogeneous supersaturation throughout the mixing zone, which in turn triggers uniform nucleation and growth of lipid aggregates into nanoscale vesicles. Compared with traditional batch methods or weakly mixed flows, the CJTM yields liposomes with smaller average diameters, lower polydispersity, and narrower size distributions at ambient temperature and without the need for high energy input or complex hardware.

In practice, the only mechanical energy required in the CJTM process derives from liquid pumping: no moving mechanical parts (e.g., blades, rotors, probes), or sonotrodes, are involved, and mixing is achieved exclusively through flow-induced turbulence in the coaxial jet. This minimal energy demand, combined with the room-temperature operating conditions and the absence of specialized microfabricated nozzles, makes the CJTM a reliable, simple, and high-throughput platform for scalable liposomal nanoparticle production. Continuous operation further enhances reproducibility and process control, key aspects of a QbD-guided workflow that ensures product quality and batch-to-batch consistency (Buttitta et al., 2024).

The efficacy of the CJTM in producing small, monodisperse vesicles contrasts with laminar or low-energy methods, where slow interdiffusion often yields broader size distributions and limited control over particle attributes. In the context of vitamin D_3-loaded nanoliposomes, this controlled turbulent mixing provides a robust foundation for subsequent process optimization, stability studies, and formulation refinement.

2.2.2. Dynamic light scattering (DLS) analysis

The hydrodynamic properties of the liposomal dispersions were characterized by Dynamic Light Scattering using a Zetasizer Pro Red Label (Malvern Instruments, UK). Measurements were carried out at 25 °C. Z-average diameter and polydispersity index (PDI) were obtained from cumulant analysis of the intensity autocorrelation function, whereas ζ-potential was determined by electrophoretic light scattering using folded capillary cells DTS1070. Each batch was measured in triplicate, and results are reported as mean ± standard deviation. For comparison, the droplet-size distribution of commercial vitamin D_3 products was additionally assessed by laser diffraction (Mastersizer 3000, Malvern Instruments), allowing qualitative benchmarking between commercial nanoliposomal suspensions and the final formulation of this work.

2.2.3. Vitamin D_3 quantification by HPLC

Vitamin D_3 content, both in the total bulk dispersion and in the permeate after ultrafiltration, was quantified by high-performance liquid chromatography (HPLC) using the Agilent 1260 Infinity system equipped with a Kinetex® XB-C18 reversed-phase column (4.6 × 150 mm, 2.6 μm; Phenomenex). Chromatographic separation was obtained under isocratic conditions with acetonitrile/water (99/1, v/v) at 1.0 mL min^{-1}, with UV detection at 265 nm, an injection volume of +40 μL, and a column temperature of 40 °C. The analyte eluted reproducibly between 7–8 min, and calibration over the range 0.5–50 μg mL^{-1} showed excellent linearity (R2 > 0.999). Encapsulation efficiency was determined after tangential-flow ultrafiltration (Minimate™ Tangential Flow Filtration Capsule of 300 kDa MWCO from Cytiva) by quantifying the vitamin D_3 concentration in the permeate (C_{perm}) and comparing it with the total vitamin D_3 concentration in the dispersion (C_{tot}). The permeate was taken as representative of the freely diffusible fraction, i.e. vitamin D_3 not retained by the liposomal structures:

$$EE(\%) = \left(1 - \frac{C_{perm}}{C_{tot}}\right) \times 100 \quad (1)$$

where (C_{tot}) and (C_{perm}) are, respectively, total vitamin D_3 concentrations and in permeate.

2.2.4. Rheological tests

To evaluate pourability and consumer handling properties, the apparent viscosity of the liposomal suspensions was measured at 25 °C using a Brookfield LVDVE rotational viscometer fitted with spindle LV-1. Prior to testing, samples were gently homogenized to avoid air entrainment while preserving vesicle integrity. Steady-shear viscosity was recorded at 60 rpm and compared with that of representative commercial vitamin D_3 products analyzed under identical conditions. This approach allowed to contextualize the rheological profile of the nanoliposomal formulation relative to market benchmarks, highlighting differences attributable to the aqueous, lipid-based matrix rather than to dosing form alone.

2.2.5. Stability tests

Stability was investigated by monitoring the evolution of both colloidal and chemical attributes under controlled storage. For the intermediate formulations (S1–S4), stability was assessed over short time windows (on the order of two weeks), sufficient to discriminate the effect of encapsulation, antioxidants, and production method on early degradation trends, consistently with the kinetic analysis discussed in Section 3.3. Measurements included Z-average, PDI, ζ-potential, and vitamin D_3 content at predefined intervals.

For the final optimized formulation, stability was followed for a substantially longer period (≈ 3–4 months), light-protected conditions, providing evidence of formulation robustness beyond the exploratory screening phase. Long-term stability data, although not shown here, were consistent with the kinetic trends and supported formulation selection and were used qualitatively to support the discussion in Appendix A. Accelerated tests at 40 °C complemented real-time storage and were interpreted using common equivalence assumptions to estimate medium-term shelf performance, always in conjunction with the kinetics derived from the short-term experiments.

2.3. Design of Experiment (DoE)

Process optimization of the coaxial-jet mixer was carried out through a response-surface Design of Experiment (DoE) prior to incorporating vitamin D_3. A three-factor, three-level Box–Behnken design (BBD) was selected to quantify how the main operating conditions, treated as factors or Critical Process Parameters (CPPs), influence the colloidal properties of the drug-free liposomal dispersions. The CPPs considered were the ethanol (solvent) stream flow rate, (Q_{IN}), the aqueous (antisolvent) stream flow rate, (Q_{OUT}), and the phosphatidylcholine concentration in the solvent phase, (C_{PC}). In the experimental matrix, (Q_{IN}) was varied between 18 and 60 mL/min, (Q_{OUT}) between 180 and 600 mL/min, and (C_{PC}) between 25 and 75 g/L, with the coded central point corresponding to 36 mL/min, 360 mL/min and 50 g/L, respectively.

The Critical Quality Attributes (CQAs), or responses, monitored for each experimental run were the Z-average diameter, the polydispersity index (PDI), and the ζ-potential of the resulting liposomal suspensions. Together, these CQAs capture vesicle size, breadth of the particle-size distribution and colloidal stability and were therefore used to evaluate

the impact of the CPPs and to delineate a suitable design space. The BBD generated 13 distinct combinations of the three CPPs, including the center point, which was replicated to provide an internal estimate of experimental variability and to allow lack-of-fit testing.

Experimental data were fitted with polynomial response-surface models. Starting from a full quadratic form, progressively simpler structures (quadratic, then linear with interactions, then purely linear) were considered, and for each response the statistically adequate model was selected based on analysis of variance (ANOVA), the coefficients of determination (R^2 and adjusted R^2), and information-criterion diagnostics. Model adequacy was further checked through lack-of-fit tests and residual-analysis (normality and homoscedasticity), ensuring that the final equations could reliably describe the behavior of the CQAs within the explored region of the CPP space (Caccavo et al., 2025).

Once validated, the models were used for numerical optimization. The target was to identify operating conditions that minimized Z-average and PDI while maintaining ζ-potential values with sufficiently high absolute magnitude ($|\zeta| \gtrsim 30$ mV) to guarantee electrostatic stabilization. The resulting optimal region, defined in terms of Q_{IN}, Q_{OUT} and C_{PC}, was then taken as the process design space for subsequent experiments with vitamin D_3, as discussed in Section 3.1.

3. Results

The results section follows the sequential development of the formulation. First, the process design space of the coaxial-jet mixer is mapped using a Box–Behnken design (Section 3.1). The identified conditions are then validated for vitamin D_3-loaded liposomes (Section 3.2), followed by a mechanistic stability study (Section 3.3) and the development of the final optimized formulation (Section 3.4). A comparison of the final optimized formulation with commercial products is reported in Appendix A, then a summary of the main results is given in Section 3.5.

3.1. Process optimization through Box–Behnken design

The first objective of the study was to identify the process conditions that control liposome formation in the coaxial-jet mixer, via DoE (Lindsay et al., 2024). For this purpose, a Box–Behnken Design (BBD) was implemented on the drug-free phosphatidylcholine system to map the relationships between process variables and the resulting liposomal characteristics.

Three Critical Process Parameters (CPPs) were varied at three levels: ethanol stream flow rate (Q_{IN}), aqueous stream flow rate (Q_{OUT}), and PC concentration (C_{PC}). The 13 experimental combinations generated by the BBD, together with the corresponding repetitions, are summarized in Table 1, which replaces the 27 experiments that would have been required by a full factorial plan.

The Critical Quality Attributes monitored (CQAs) were: Z-average diameter, PDI, and ζ-potential, as already stated in previous section. These descriptors jointly capture vesicle size, size distribution breadth, multimodality and colloidal stability.

It should be emphasized that the experimental responses reported in Table 1 correspond to the full set of conditions explored within the Box–Behnken design and therefore include combinations located at the boundaries of the investigated process space. In a Quality-by-Design framework, these boundary points are intentionally included to allow reliable mapping of the response surfaces and to identify the operating region where the desired critical quality attributes can be achieved. Consequently, some responses obtained under extreme conditions (e.g., very small Z-average values, unusually high absolute ζ-potentials, or broad PDI values) should be interpreted as exploratory outcomes of the screening design rather than as target formulations. The optimized operating window identified by the response-surface analysis corresponds instead to the region where liposomes exhibit sizes, dispersion characteristics, and electrostatic stability consistent with technologically relevant systems, as discussed in the subsequent sections.

Except for these boundary values, Z-average values remained within the SUV domain (≈30–70 nm), ζ-potential ranged from about −30 to −60 mV, and PDI values indicated systems spanning moderately to broadly dispersed populations. With reference to the highest values of PDI, scarcely acceptable, these values were restricted to combinations at the edges of the design space and were not observed in optimized regions.

Polynomial response-surface models were built for each response following a top-down strategy: quadratic → linear with interactions → linear without interactions, selecting at each step the statistically adequate structure according to ANOVA, R^2/R^2adj, PRESS and AICc criteria. Across responses, significant terms and final model structure differed, but all retained satisfactory predictive ability in the explored domain. These procedures are fully consistent with the methodological framework discussed in the supporting sources.

The response-surface plots in Fig. 1, obtained at the central level of the third factor, provide a compact visualization of the main trends:

- Z-average decreased at higher Q_{IN}, while increasing C_{PC} concentration systematically produced larger vesicles, as already known from

Table 1
Box–Behnken experimental design used to investigate the influence of process variables on the formation of drug-free phosphatidylcholine liposomes in the coaxial-jet mixer. The three investigated factors (Critical Process Parameters, CPPs) were the solvent stream flow rate (Q_{IN}), the antisolvent stream flow rate (Q_{OUT}), and the phosphatidylcholine concentration in ethanol (C_{PC}). Each factor was evaluated at three coded levels (−1, 0, +1) corresponding to the operating conditions reported in the table. The measured responses (Critical Quality Attributes, CQAs) were the Z-average hydrodynamic diameter, polydispersity index (PDI), and ζ-potential, determined by dynamic light scattering (Caccavo et al., 2025).

	Levels			Factors			Responses		
Run #	Q_{IN} …	Q_{OUT} …	C_{PC} …	Q_{IN} mL/min	Q_{OUT} mL/min	C_{PC} g/L	Z-average nm	PDI …	ζ-potential mV
1	0	0	0	36	360	50	26.6 ± 6.6	0.49 ± 0.68	−60.4 ± 4.8
2	+1	+1	0	60	600	50	25.7 ± 6.6	0.45 ± 0.03	−60.5 ± 10.8
3	−1	−1	0	18	180	50	31.6 ± 6.6	0.74 ± 0.22	−65.6 ± 10.3
4	−1	+1	0	18	600	50	29.1 ± 1.3	0.56 ± 0.13	−42.1 ± 8.8
5	+1	−1	0	60	180	50	23.2 ± 1.8	0.54 ± 0.00	−72.6 ± 1.5
6	−1	0	−1	18	360	25	42.0 ± 10.1	0.35 ± 0.04	−32.8 ± 4.5
7	+1	0	−1	60	360	25	11.3 ± 1.9	0.67 ± 0.10	−37.7 ± 1.9
8	0	−1	−1	36	180	25	17.8 ± 4.1	0.51 ± 0.00	−38.6 ± 2.7
9	0	+1	−1	36	600	25	12.9 ± 1.2	0.82 ± 0.17	−30.8 ± 4.6
10	−1	0	+1	18	360	75	53.3 ± 3.1	0.48 ± 0.06	−48.3 ± 9.3
11	+1	0	+1	60	360	75	36.7 ± 0.8	0.49 ± 0.17	−55.6 ± 19.8
12	0	−1	+1	36	180	75	45.6 ± 3.2	0.44 ± 0.03	−60.1 ± 9.0
13	0	+1	+1	36	600	75	33.0 ± 1.8	0.54 ± 0.03	−46.1 ± 4.1

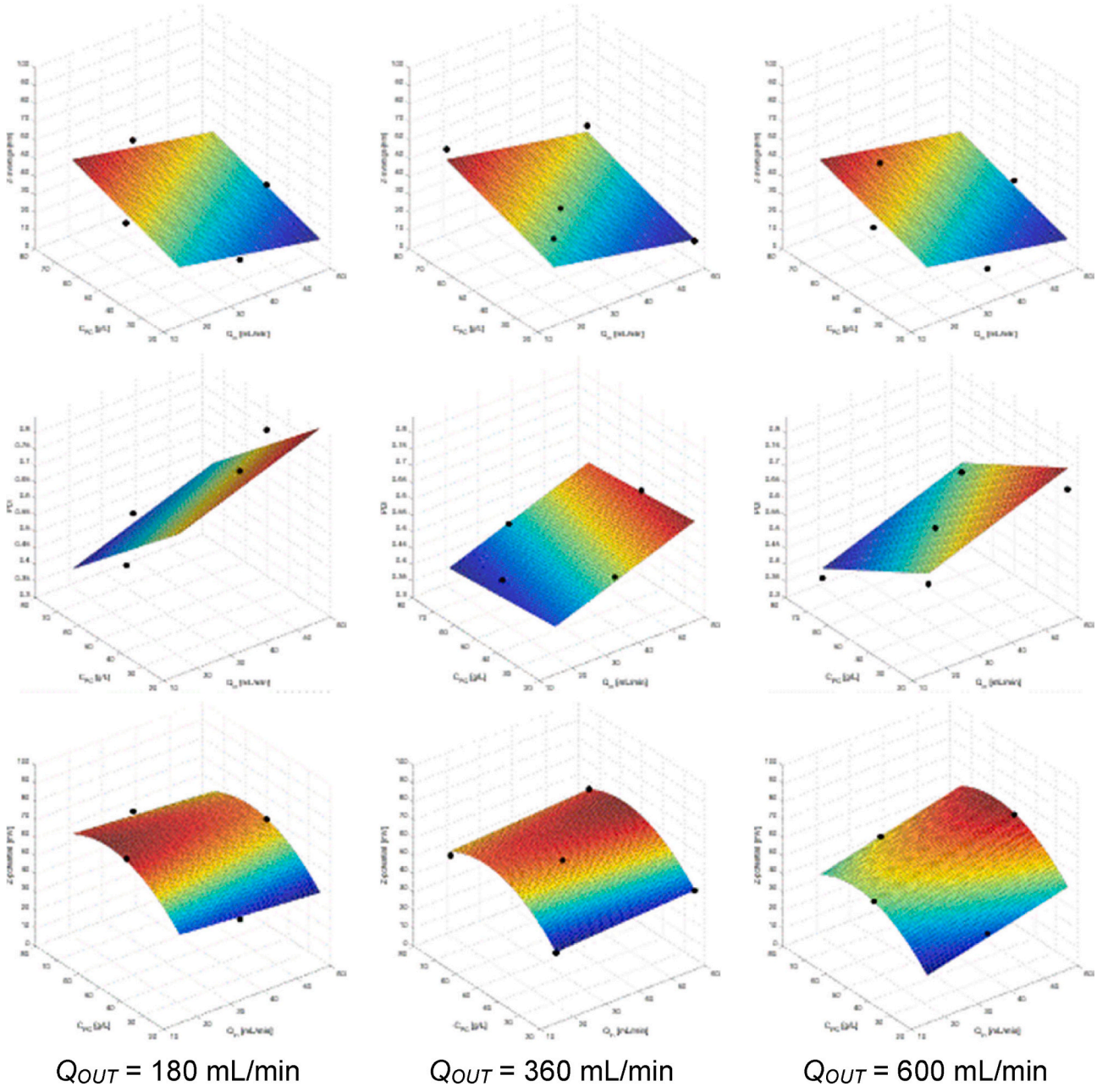

Fig. 1. Response-surface plots illustrating the influence of the main process variables on the critical quality attributes of drug-free liposomal dispersions obtained through the Box–Behnken design. The surfaces show the predicted variation of Z-average diameter (top row), polydispersity index (middle row), and ζ-potential (bottom row) as a function of the solvent stream flow rate (Q_{IN}) and phosphatidylcholine concentration (C_{PC}). Each column corresponds to a different value of the antisolvent flow rate Q_{OUT} (180, 360, and 600 mL min^{-1}, respectively). Color gradients represent the magnitude of the predicted response obtained from the fitted response-surface models. These plots visualize the combined effects of hydrodynamic conditions and lipid concentration on liposome size, dispersion uniformity, and electrostatic stability.

Barba et al. (2017). The effect of Q_{OUT} was comparatively weaker, appearing only as a secondary modulation.

- PDI tended to decrease at intermediate-to-high Q_{OUT}, whereas high concentration favored narrower distributions only within specific combinations, consistent with the onset of multimodality at extremes.
- ζ-potential increased in absolute value with C_{PC} concentration up to an intermediate level, beyond which partial reduction was observed, plausibly due to charge masking and enhanced aggregation propensity at very high solids.

These observations confirm that Q_{IN} and C_{PC} concentration are the primary levers of nano-structuring, while Q_{OUT} mainly acts as a fine tuner.

The complete dataset generated by the BBD (Z-average, PDI, ζ-potential for all 13 runs) is already represented numerically within the model-fitting workflow and graphically condensed in Table 1 and Fig. 1. The models cover the entire experimental domain and therefore allow interpolation across combinations, avoiding the need to display every measured point in separate plots.

For clarity and reproducibility, the following results are explicitly highlighted:

- minimum Z-average values occur at high Q_{IN} / low C_{PC} concentration

- maximum $|\zeta|$ values are obtained at moderate–high concentration, with limited sensitivity to Q_{OUT}
- multimodality (high PDI + divergent MIPS) emerges when high concentration coincides with low mixing intensity

These behaviors will be essential when vitamin D_3 is introduced (following section 3.2), since the drug may shift size distributions or destabilize the bilayer; having an established drug-free design space enables us to distinguish matrix effects from drug-induced ones.

Within the investigated range, the BBD-derived models define a region where the process reproducibly yields small, stable liposomes. Acceptable CQAs are achieved when:

- Q_{IN} is maintained at medium–high values,
- C_{PC} concentration is kept at low–medium levels, and
- Q_{OUT} is not at its lowest level.

Under these conditions, Z-average remains below ≈60 nm, PDI is minimized, and $|\zeta|$ exceeds ~30 mV, ensuring electrostatic stabilization.

This operating window is used as the reference design space for subsequent experiments where vitamin D_3 is incorporated.

It should be noted that the Box–Behnken design reported in this section was intentionally performed on the drug-free phosphatidylcholine system to isolate the effects of the process variables on liposome formation. Within a Quality-by-Design framework, this step aims at identifying the relationships between mixing conditions, lipid concentration, and the resulting vesicle characteristics, thereby defining a robust operating window for nanoscale liposome production. The subsequent experiments involving vitamin D_3 (Section 3.2) were carried out using conditions selected from this process space. Because the presence of a lipophilic payload can influence bilayer packing and vesicle growth dynamics, the resulting particle sizes may differ from those observed in the drug-free screening system. For this reason, Table 1 should be interpreted as a process-mapping tool rather than as a direct predictor of the final formulation characteristics.

This two-step approach (drug-free process mapping followed by payload validation) is commonly adopted in nanoparticle formulation studies to disentangle hydrodynamic effects from drug–matrix interactions.

3.2. Bridging validation with vitamin D_3

Once the process design space had been identified in the drug-free system, the next step was to verify its transferability to vitamin D_3-loaded liposomes. Therefore, to verify that the process window identified in the drug-free system (Section 3.1) remains suitable when a lipophilic payload is incorporated, vitamin D_3 was co-formulated with phosphatidylcholine (PC) and processed under controlled hydrodynamic conditions. These experiments therefore serve as a practical validation step of the design space identified in the drug-free system, allowing verification that the hydrodynamic trends governing liposome formation remain qualitatively valid after incorporation of the lipophilic payload.

Three ethanol solutions (Recipes #1–#3) were prepared, in which vitamin D_3 were fixed at 10 % w/w of PC. PC concentrations in ethanol were 94, 44 and 24 g/L, corresponding in the final product to PC levels of approximately 8.6, 4.0 and 2.4 g/L and proportional vitamin D_3 contents. Liposomes were then produced at three inner/outer flow-rate pairs representative of laminar, transitional and fully turbulent regimes in the coaxial jet: 4.5/45, 19/193 and 36/360 mL/min, respectively. These conditions span an average mixing Reynolds number $N_{Re_{mix}} = \frac{4\dot{Q}_{mix}}{\pi D \nu_{mix}}$ from ≈ 240 (laminar), to ≈ 1032 (transition), to ≈ 1920 (turbulent). Higher Reynolds numbers mean faster local mixing, which suppresses vesicle growth. At same time, these conditions maintain a nearly constant Flow Momentum Ratio ($FMR = (\rho v)_{in}/(\rho v)_{out} = 5.9$) and Flow Velocity Ratio ($FVR = v_{in}/v_{out} = 7.5$), so that changes in hydrodynamics primarily affect micromixing time rather than overall composition (Caccavo et al., 2023). A concise summary of recipes and operating conditions, together with the measured Z-average, PDI and encapsulation efficiency (EE%), is reported in Table 2.

Across all formulations and flow regimes, EE% remained very high (≈ 99 %), with no dependence on the hydrodynamic condition. Increasing PC concentration, and thus vitamin D_3 loading, did not compromise encapsulation, confirming the strong affinity of this lipophilic drug for the phospholipid bilayer and the robustness of the tangential-flow purification method.

Dynamic Light Scattering showed that particle size and distribution breadth were instead sensitive to both composition and micromixing intensity, as reported in Fig. 2 (both intensity-based and volume-based particle size distributions derived from the DLS measurements are reported). At the highest PC concentration (94 g/L), liposomes were consistently larger than those obtained at 44 and 24 g/L, regardless of the flow regime, indicating a tendency toward vesicle growth and aggregation at very high solid content. Conversely, no appreciable differences in Z-average were observed between the medium and low PC levels, suggesting that, within this range, hydrodynamics rather than composition becomes the dominant control variable.

Within each recipe, Z-average decreased as the mixing Reynolds number increased from laminar to turbulent conditions, i.e. as the characteristic mixing time τ_{mix} shortened from the order of seconds to a few tens of milliseconds. This trend mirrors the behavior observed in the drug-free Box–Behnken study and confirms that faster micromixing quenches nucleation and early growth more efficiently, leading to smaller vesicles at comparable composition.

The corresponding particle-size distributions (PSD) further highlight the role of hydrodynamics.

Both intensity-based and volume-based particle size distributions derived from the DLS measurements are reported in Fig. 2 (upper and lower right panels, respectively). The intensity distribution represents the primary signal obtained from dynamic light scattering and is particularly sensitive to larger scattering objects, whereas the volumetric distribution is obtained through standard post-processing algorithms and provides a representation that is often easier to interpret in terms of relative particle populations. Presenting both representations allows a more transparent inspection of the data and facilitates comparison between the different fluid-dynamic regimes investigated in this work. Under laminar conditions, PSDs were broader and, in some cases, slightly multimodal, reflecting a wider spectrum of nucleation and growth histories. Transition and turbulent regimes produced visibly narrower, more symmetric PSDs, with the turbulent case delivering the tightest distributions and the best control over mean size. In the turbulent regime, the intensity distribution exhibits a dominant single peak with reduced tailing toward larger diameters compared with the laminar

Table 2
Composition of ethanol feed solutions and corresponding hydrodynamic conditions used for the preparation of vitamin D_3-loaded liposomes. The left part of the table reports the phosphatidylcholine concentration (C_{PC}), the corresponding vitamin D_3 concentration (C_{D3}), and the measured encapsulation efficiency (EE%). The right part reports the solvent (Q_{IN}) and antisolvent (Q_{OUT}) flow rates and the resulting mixture Reynolds number (Remix) characterizing the micromixing regime in the coaxial-jet mixer. In all formulations the drug loading ratio was fixed at $C_{D3} = 10\ \%C_{PC}$ (w/w). Flow rates were selected to maintain approximately constant flow momentum ratio (FMR ≈ 5.9) and flow velocity ratio (FVR ≈ 7.5), while varying the Reynolds number to span laminar, transitional, and turbulent mixing regimes.

C_{PC} g/L	C_{D3} g/L	EE %	Q_{IN} mL/min	Q_{OUT} mL/min	$N_{Re_{mix}}$ …
94	9.4	99.8	4.5	45	240
44	4.4	99.5	19	193	1032
24	2.4	99.6	36	360	1920

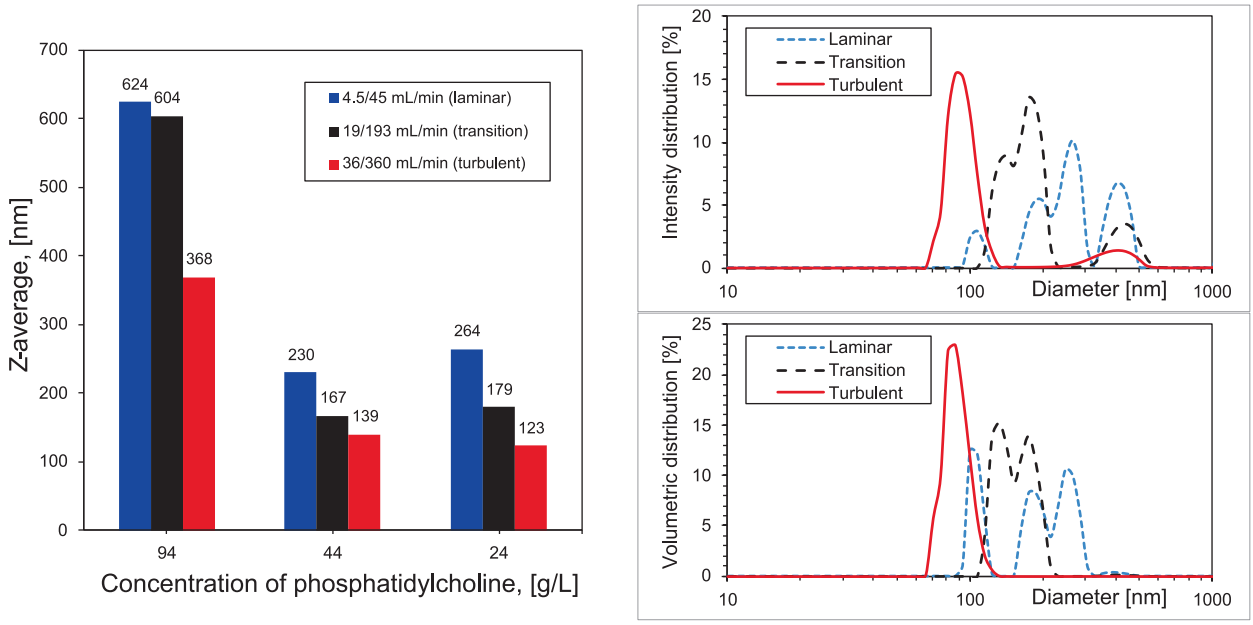

Fig. 2. Effect of lipid concentration and micromixing regime on the size of vitamin D_3-loaded nanoliposomes produced by the coaxial-jet mixer. Left panel: Z-average hydrodynamic diameter obtained by dynamic light scattering as a function of phosphatidylcholine concentration in ethanol (94, 44, and 24 g L^{-1}) under three different hydrodynamic regimes corresponding to laminar (Q_{IN}/Q_{OUT} = 4.5/45 mL min^{-1}), transitional (19/193 mL min^{-1}), and turbulent (36/360 mL min^{-1}) mixing conditions (laminar = blue, transition = black, turbulent = red, even in the right panels). Increasing micromixing intensity (higher Reynolds number) leads to progressively smaller vesicles. Right panels: Particle-size distributions of liposomes prepared at C_{PC} = 24 g L^{-1} under the same three hydrodynamic regimes. The upper plot shows the intensity-weighted distribution, which corresponds to the primary signal obtained from dynamic light scattering and is particularly sensitive to larger scattering particles. The lower plot shows the corresponding volume-weighted distribution obtained through standard post-processing of the DLS signal. Comparison between regimes highlights the narrowing of the particle population under turbulent mixing conditions.

and transitional conditions, indicating a substantially narrower particle population. While dynamic light scattering cannot strictly demonstrate perfect monodispersity, these results indicate that intense micromixing promotes the formation of a more uniform vesicle population. This behavior is consistent across Recipes #2 and #3 and, although less pronounced at the highest PC concentration, still supports the beneficial effect of intense micromixing on colloidal uniformity, as confirmed also by literature (Akar et al., 2024).

Taken together, these results define a practical design space for vitamin D_3-loaded nanoliposomes: when PC concentrations in the final dispersion are kept at or below ≈ 4–8 g/L and the coaxial-jet mixer operates at $N_{Re_{mix}} \geq 103$ (transition/turbulent regime with $Q_{IN} \approx$ 19–36 mL/min and $Q_{OUT} \approx$ 193–360 mL/min), the process reproducibly yields high-EE% (≈ 99 %), sub-200 nm liposomes with narrow PSDs. This subset of conditions, centered on the turbulent regime at 36/360 mL/min, was therefore selected as the operating window for the subsequent stability studies (Section 3.3) and for the preparation of the product used in the comparative benchmarking against commercial references (Appendix A).

Importantly, the results highlight how controlled micromixing conditions can be used to systematically relate process parameters to vesicle characteristics and formulation stability, with the formulation emerging as a consequence of the identified design space rather than as the result of empirical trial-and-error.

3.3. Stability and degradation kinetics in alternative formulation scenarios

After validating liposome formation with vitamin D_3, a mechanistic stability study was performed to disentangle the respective roles of liposomal encapsulation, antioxidant protection, and micromixing conditions. Therefore, the physicochemical stability and degradation kinetics of vitamin D_3 in four aqueous formulations differing in lipid encapsulation, antioxidant content, and production method have been compared. This dataset provides an important mechanistic bridge between the initial encapsulation experiments (Section 3.2) and the final product benchmarking (Appendix A), helping clarify the relative contribution of each formulation element – liposomes, antioxidants, and micromixing – to long-term stability.

3.3.1. Formulations and study design

Four model solutions (S1–S4) were prepared to isolate the effect of key variables:

- S1 – Liposomal D_3, no antioxidant, coaxial-jet mixer
- S2 – Liposomal D_3 + sodium ascorbate (antioxidant), coaxial-jet mixer
- S3 – Liposomal D_3 + sodium ascorbate (antioxidant), mixing by magnetic stirrer
- S4 – Non-liposomal D_3 + sodium ascorbate (antioxidant), coaxial-jet mixer

This design enables dissection of:

i. the protective effect of liposomal encapsulation;
ii. the contribution of antioxidants;
iii. the importance of high-energy micromixing in achieving robust vesicle formation.

All solutions were stored at 25, 40, and 65 °C and monitored over time via DLS (particle size stability) and HPLC (quantitative D_3 retention). Full kinetic analyses were performed using the integral method to identify the reaction order (order 0 vs. order 1), revealing a two-stage degradation model, as detailed below.

3.3.2. Particle-size stability and role of micromixing

DLS confirmed that the coaxial jet mixer produced markedly smaller and more uniform liposomes than manual mixing. Liposomes in S1 and

S2 (coaxial-jet prepared systems) showed initial Z-average values of ~30–35 nm, stable over 20 h, whereas S3 liposomes (manual mixing) were noticeably larger (~85–90 nm) (Fig. 3). These data corroborate the dominant role of turbulent micromixing in controlling nucleation and bilayer assembly, consistent with the process-driven findings in Section 3.1. Furthermore, the presence of antioxidants seems to confer to the liposome some sort of thermal stability (formulation S1 noticeably increases its size after 23 h at 65 °C). The degradation kinetics corresponding to these formulations are analyzed in the following subsection.

3.3.3. Stability and degradation kinetics

Fig. 4 reports the normalized concentration profiles (C_a/C_{a0}) as a function of time for the four formulations (S1–S4) stored at 25, 40 and 65 °C. Independently of formulation, degradation accelerated with increasing temperature, as expected for thermally driven reactions. However, clear formulation-dependent differences emerged.

At 65 °C, S4 (no liposomes) showed the fastest decay, with a rapid drop of C_a/C_{a0} to nearly zero within the first tens of hours. The presence of phosphatidylcholine markedly slowed degradation, as seen in S1–S3. Among these, S2 (liposomes + antioxidant, COAX) provided the best stabilization across all temperatures, whereas S1 (no antioxidant) exhibited intermediate behavior, confirming the protective role of the antioxidant. S3 (manual mixing) was systematically less stable than S2, indicating that the combination of controlled micromixing (likely via more homogeneous vesicle formation) and antioxidant protection contributes to improved preservation. Summarizing, the comparison between S1–S4 indicates that the improved stability observed in the optimized formulation arises from the combined action of structural and chemical stabilization mechanisms. The antioxidant system directly reduces oxidative degradation of vitamin D_3, whereas the micromixing conditions achieved in the coaxial-jet mixer influence vesicle formation, size distribution, and bilayer uniformity. The intermediate behavior of the manually mixed formulation (S3) suggests that antioxidants alone can partially mitigate degradation, but that the structural homogeneity obtained under intense micromixing further enhances the protective effect of the liposomal environment. These observations therefore support the view that micromixing and antioxidant protection act synergistically rather than independently in determining the overall stability of the system.

The degradation curves were interpreted using batch kinetic models. For all formulations, the time courses were best described by the superposition of two zero-order processes operating sequentially, each characterized by a different apparent rate constant. Alternative kinetic formulations have also been found to be able to describe the data; the zero-order model was chosen for sake of interpretability and for the higher values of Pearson's coefficient. At short times, a faster contribution dominates, whereas at longer times the degradation proceeds more slowly. This suggests the coexistence of at least two mechanisms, plausibly associated with (i) readily accessible vitamin D_3 fractions and (ii) fractions progressively released or exposed during storage.

A possible mechanistic interpretation of this behavior is related to the heterogeneous localization of vitamin D_3 within the phospholipid bilayer. Lipophilic molecules such as cholecalciferol can occupy different positions within the membrane, ranging from regions close to the lipid–water interface to deeper locations within the hydrophobic core of the bilayer. Molecules located near the interfacial region are more exposed to oxygen and to the surrounding aqueous environment and therefore may undergo degradation more rapidly, contributing to the initial faster kinetic regime. In contrast, molecules embedded deeper in the bilayer experience a more hydrophobic and less reactive environment, resulting in slower degradation rates that dominate at longer storage times. In addition, slow bilayer reorganization or partial release of vitamin D_3 during storage may progressively shift molecules between these environments, producing the observed transition between the two apparent kinetic regimes. Similar multi-phase degradation behaviors have been reported for lipophilic antioxidants and vitamins incorporated in lipid-based formulations, where differences in molecular localization within the lipid phase lead to different effective oxidation environments (Musakhanian et al., 2022).

To facilitate comparison while limiting the number of figures, the kinetic parameters obtained for each system and temperature (previously reported separately) are condensed in Table 3. The table clearly highlights that:

- rate constants increase with temperature for all systems;
- at each temperature, k-values follow the trend S1 > S4 > S3 > S2, confirming the combined protective role of both antioxidant and liposomal encapsulation;
- the coaxial-jet formulations systematically outperform the manually prepared ones.

The comparison across formulations shows that the degradation rate in S4 is always the highest, underscoring the intrinsic instability of vitamin D_3 in aqueous media even in the presence of antioxidant.

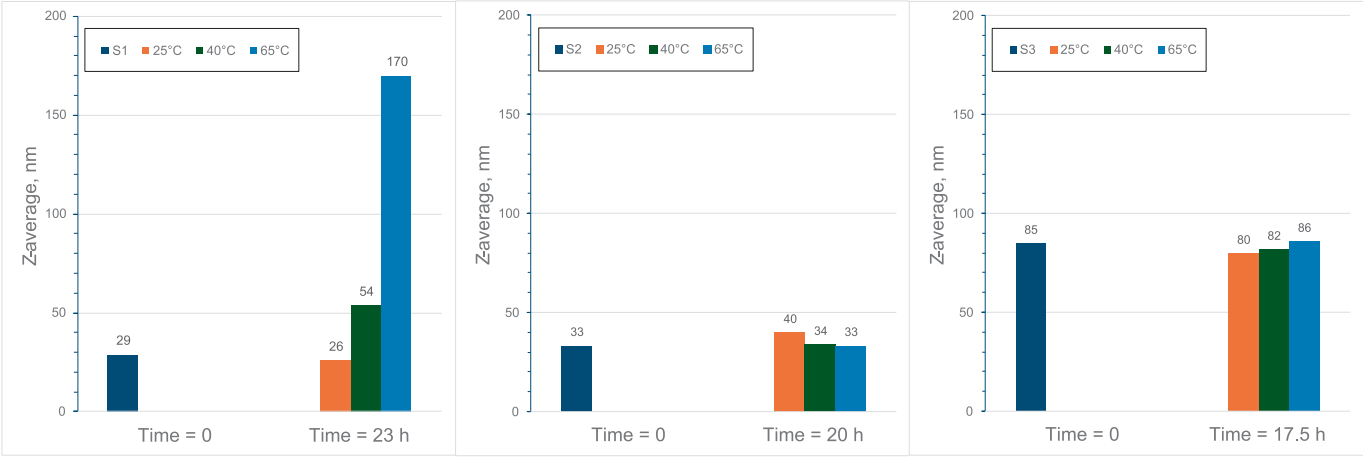

Fig. 3. Comparison of liposome size obtained under different formulation and preparation conditions. The Z-average hydrodynamic diameter measured by dynamic light scattering is reported at t = 0 and after approximately 20 h of storage at different temperatures for three liposomal systems: S1: liposomal vitamin D_3 prepared by coaxial-jet mixing without antioxidant; S2: liposomal vitamin D_3 prepared by coaxial-jet mixing in the presence of sodium ascorbate; S3: liposomal vitamin D_3 prepared by conventional magnetic stirring in the presence of sodium ascorbate. The data illustrate the influence of both antioxidant protection and micromixing intensity on vesicle stability. Liposomes produced by the coaxial-jet mixer (S1 and S2) exhibit smaller initial sizes and improved stability compared with those obtained by manual mixing (S3), while the presence of antioxidant further mitigates thermally induced destabilization.

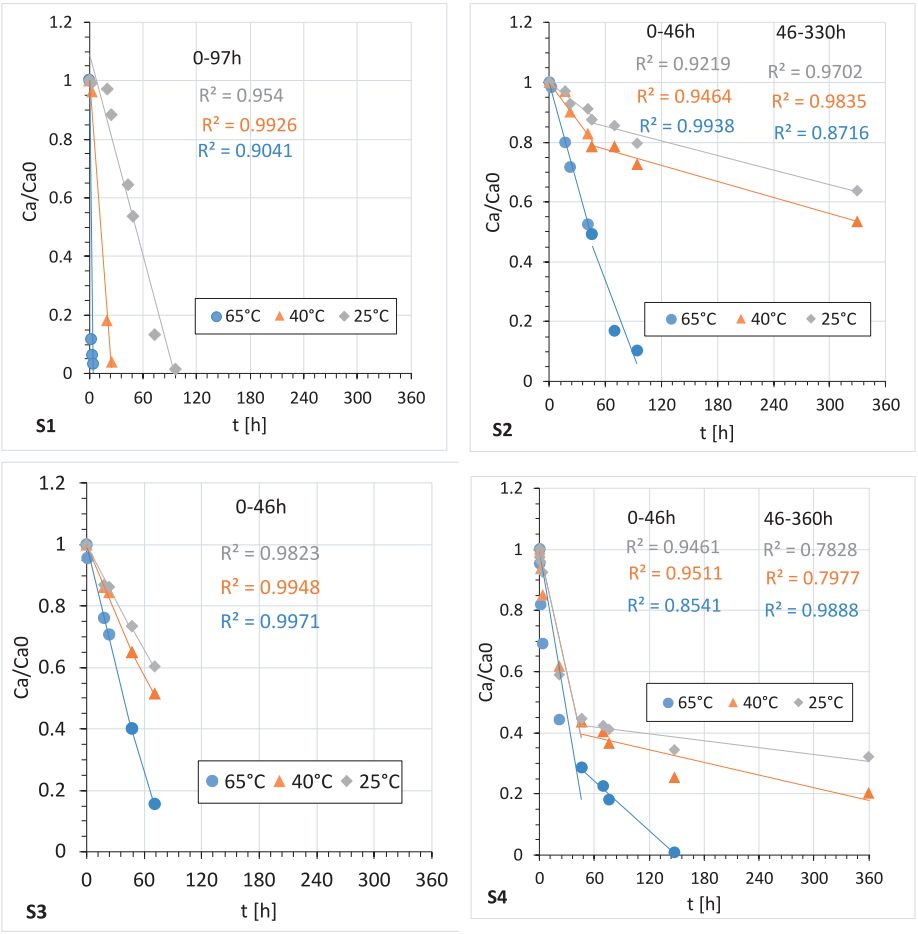

Fig. 4. Thermal degradation kinetics of vitamin D_3 in four model aqueous formulations differing in encapsulation, antioxidant presence, and preparation method. Each panel corresponds to one formulation: S1 (liposomal vitamin D_3, no antioxidant, prepared by coaxial-jet mixing), S2 (liposomal vitamin D_3 with sodium ascorbate, coaxial-jet mixing), S3 (liposomal vitamin D_3 with sodium ascorbate, prepared by magnetic stirring), and S4 (non-liposomal vitamin D_3 with sodium ascorbate). The normalized vitamin concentration (C_a/C_{a0}) is plotted as a function of time for storage at 25 °C (gray diamonds), 40 °C (orange triangles), and 65 °C (blue circles). Solid lines represent kinetic fits obtained using a two-stage zero-order degradation model. The separation between short- and long-time regimes (indicated in each panel) reflects the transition between two apparent degradation processes. The comparison highlights the strong stabilizing effect of liposomal encapsulation and antioxidant addition, with the coaxial-jet formulation containing antioxidant (S2) providing the slowest degradation across all temperatures.

Table 3
Apparent zero-order degradation rate constants for vitamin D_3 obtained from the kinetic analysis of the concentration profiles shown in Fig. 4. Two sequential kinetic regimes were identified for each formulation: an initial short-time regime characterized by rate constant $k_{i,1}$, followed by a long-time regime characterized by rate constant $k_{i,2}$. Rate constants are expressed in μg mL^{-1} h^{-1} and are reported for the four investigated formulations: S1 (liposomal vitamin D_3 without antioxidant, coaxial-jet mixing), S2 (liposomal vitamin D_3 with antioxidant, coaxial-jet mixing), S3 (liposomal vitamin D_3 with antioxidant, magnetic stirring), and S4 (non-liposomal vitamin D_3 with antioxidant). Measurements were performed at 25 °C, 40 °C, and 65 °C.

	$T = 25$ °C		$T = 40$ °C		$T = 65$ °C	
	$k_{i,1}$	$k_{i,2}$	$k_{i,1}$	$k_{i,2}$	$k_{i,1}$	$k_{i,2}$
S1	0.13	0.24	0.77	…	4.44	…
S2	0.07	0.02	0.11	0.02	0.30	0.22
S3	0.12	0.11	0.15	0.12	0.27	0.21
S4	0.34	0.01	0.34	0.02	0.45	0.07

Encapsulation in liposomes reduces the rate substantially (S1), while the addition of antioxidant further decreases it (S2). The manually prepared suspension (S3) exhibits intermediate behavior between S1 and S2, confirming the additional benefit introduced by the coaxial-injection method. Overall, the most favorable condition is consistently obtained for S2, which displays the slowest degradation at all temperatures tested.

3.4. *Novel formulation and stability*

Based on the mechanistic insights obtained in Section 3.3, the formulation strategy was refined to develop the final optimized nano-liposomal vitamin D_3 product. From the work done in the previous Section 3.3, three conclusions emerge:

- Liposomal encapsulation is necessary but not sufficient: without antioxidants (S1), degradation remains significant, especially at elevated temperatures.
- Antioxidant addition is highly synergistic with encapsulation: S2 systematically shows the lowest degradation rates at all temperatures.
- Micromixing quality determines liposome robustness: S3, despite similar composition to S2, performs markedly worse, highlighting the role of vesicle in protecting D_3.

These findings reinforce the framework adopted in our final formulation:

- tightly controlled nanoscale liposome formation (via coaxial jets),

- inclusion of an optimized antioxidant/buffer system,
- minimization of excipient load without sacrificing stability.

The intermediate kinetic study therefore provides the mechanistic rationale linking the engineering choices of Section 3.2 to enhanced technological performance of the optimized formulation shown in Appendix A.

Building on the results obtained in the stability study, formulation S2 was selected as the technological benchmark and subsequently refined with the explicit objective of developing a a technologically robust formulation. The optimization focused on improving compositional robustness, regulatory compatibility and manufacturability, while preserving the nanoliposomal architecture and stability advantages demonstrated in Section 3.3. The final formulation, described in detail in (Lamberti et al., 2025) and derived from S2 through targeted adjustments of the aqueous excipient system and antioxidant balance, is reported therein and forms the object of the comparative evaluation presented in Appendix A. The final formulation of the product includes, beyond water, ethanol, PC and vitamin D_3, also α-tocopherol and sodium ascorbate as antioxidants, citric acid and sodium citrate as pH regulators (buffer), sodium benzoate and potassium sorbate as preservers, and saccharose as taste regulator. Its stability has been studied, and the main findings are reported below; the overall performance of the product has been compared with commercial products, and results are given in Appendix A.

Fig. 5 shows the long-term stability of the optimized liposomal vitamin D_3 formulation stored at 25 °C (open blue symbols) and 40 °C (filled orange symbols), expressed as normalized vitamin D_3 content (C_a/C_{a0}, left axis, circles) and Z-average particle size (right axis, squares). Over 293 days at 25 °C and 166 days at 40 °C, the vitamin D_3 assay remains essentially unchanged ($C_a/C_{a0} \approx 1$) and the Z-average shows only minor variations (≈ 80–100 nm), indicating stable chemical and physical CQAs with no evidence of degradation or colloidal instability.

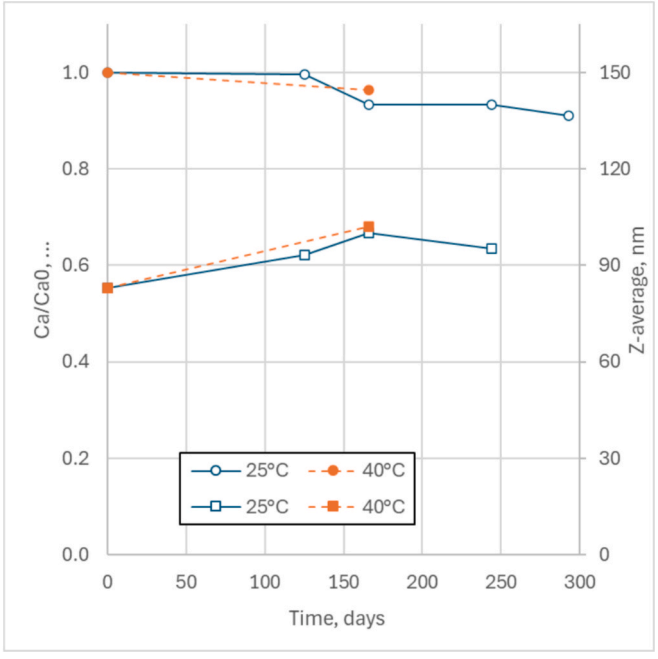

Fig. 5. Long-term stability of the optimized nanoliposomal vitamin D_3 obtained through coaxial-jet mixing. The normalized vitamin D_3 concentration (C_a/C_{a0}, circles, left axis) and the liposome Z-average hydrodynamic diameter (squares, right axis) are reported as a function of storage time under two temperature conditions: 25 °C (blue lines, hollow symbols) and 40 °C (orange lines, filled symbols). Measurements extend up to ≈293 days at 25 °C and ≈166 days at 40 °C.

Taking Q_{10} as the temperature coefficient which describes the ratio between the reaction rates (r_2/r_1) or between the times needed to obtain a certain conversion (t_1/t_2), at two temperatures (T_2 and T_1) (i.e., Q_{10} is a measure of the sensitivity to the temperature of the reaction rate, $Q_{10} = 2$ means that the reaction rate doubles for a change in temperature of 10 °C):

$$Q_{10} = \left(\frac{r_2}{r_1}\right)^{\frac{10^\circ C}{T_2 - T_1}} = \left(\frac{t_1}{t_2}\right)^{\frac{10^\circ C}{T_2 - T_1}} \quad (2)$$

For a dilute liposomal system $Q_{10} = 3$ is a reasonable and conservative sensitivity scenario, therefore a negligible concentration decay after 166 days at 40 °C means that the equivalent time at 25 °C would be $t_{25^\circ C} = t_{40^\circ C} Q_{10}^{(40-25)/10} = 863$days (28 months). On this basis, the absence of significant change under accelerated conditions supports extrapolative reasoning toward a 24-month shelf-life, complemented by ongoing real-time stability data in line with regulatory expectations (ICH Q1A, 2003).

3.5. Summary of key findings

Coaxial-jet fluido-dynamics and lipid concentration are the principal drivers of nanoscale liposome formation.
The optimized conditions identified by the BBD yield sub-100 nm, monodisperse, stable vesicles reproducibly.
Inclusion of vitamin D_3 does not alter process dynamics and provides nearly quantitative encapsulation.
The final product outperforms all tested commercial formulations in particle size, uniformity, viscosity, and dose accuracy (see Appendix A).

A comparative analysis with several commercially available aqueous "liposomal" vitamin D3 formulations was also performed in order to place the physicochemical characteristics of the present system within a broader technological context. Because this comparison is intended only as an exploratory benchmark rather than as a central element of the formulation study, the detailed results are reported in Appendix A. This additional information provides a qualitative reference frame for particle-size distributions, rheological properties, and compositional consistency observed in existing market products.

4. Discussion

4.1. Interpreting the design space: fluid dynamics and liposome formation

The experimental design confirmed that micromixing intensity – represented by the solvent-stream flow rate (Q_{IN}) – is the dominant variable controlling liposome size and homogeneity. Higher Q_{IN} enhances turbulence and reduces mixing time below the nucleation–growth timescale, leading to instantaneous supersaturation and rapid phospholipid self-assembly into nanosized vesicles.

This observation is consistent with the Damköhler-based framework of (Patterson et al., 2003) and the theoretical predictions for nanoprecipitation under turbulent jet conditions (Lim et al., 2014; Saad and Prud'homme, 2016). In contrast, high lipid concentrations increase local viscosity and diffusion limitation, widening the size distribution – an effect already observed in similar antisolvent precipitation systems for polymeric nanoparticles. The resulting trade-off between concentration and micromixing defines a narrow operating window that can be conveniently captured by the Box–Behnken response surfaces.

The bridging experiments demonstrated that the inclusion of a lipophilic active (vitamin D_3) does not significantly perturb these fluid-dynamic relationships. This confirms that the process is drug-agnostic for bilayer-incorporated actives, allowing predictable scale-up and transfer to other pharmaceuticals or lipophilic drugs. The excellent agreement between DoE-predicted and measured Z-averages (bias < 5

%) substantiates the reproducibility and robustness of the coaxial-jet system.

Particle size and dispersion characteristics in this study were primarily evaluated through dynamic light scattering, which provides rapid and statistically robust information on hydrodynamic diameter and distribution breadth for colloidal systems. The combination of Z-average, PDI, and ζ-potential measurements allowed a consistent comparison of the liposomal dispersions obtained under different hydrodynamic regimes. Imaging techniques such as cryogenic transmission electron microscopy could provide complementary structural information on vesicle morphology and lamellarity. However, the present work focuses on the process-driven control of nanoscale liposome formation within a Quality-by-Design framework, where DLS-derived parameters represent the primary critical quality attributes used to evaluate the outcome of the formulation process. In addition, the nanoscale dimensions observed are consistent with the hydrodynamic behavior expected for phospholipid vesicles formed through rapid antisolvent mixing.

Beyond the specific case of vitamin D_3 encapsulation, the present results highlight how controlled micromixing conditions can be systematically connected to vesicle architecture within a Quality-by-Design framework. While both coaxial mixing approaches and liposomal formulations have been previously reported, the integration of hydrodynamic control, response-surface modeling, and formulation stability analysis provides a clearer view of how process parameters translate into critical quality attributes such as vesicle size, dispersion uniformity, and colloidal stability. In this sense, the present study contributes to bridging the gap between nanoparticle production methods and formulation-oriented design, showing how process conditions can be used not only to produce nanoscale liposomes but also to rationalize their physicochemical behavior.

4.2. Physicochemical stability and encapsulation efficiency

The combination of phosphatidylcholine matrix (Pasarin et al., 2023; Yi et al., 2023) and α-tocopherol creates a protective environment for vitamin D_3, minimizing oxidative and photolytic degradation (Sainaga Jyothi et al., 2022). Tocopherol acts both as a membrane stabilizer and radical scavenger, while the citric/ascorbate buffer maintains a mildly acidic pH (4.5–5.5), reducing epimerization and hydrolysis.

Encapsulation efficiencies approaching 99 % are among the highest reported for vitamin D_3 liposomes, comparable only to recent microfluidic systems (Dałek et al., 2022; Żurek et al., 2023). The ζ-potential values (≈ –48 mV) exceed the empirical stability threshold (|30 mV|), preventing aggregation without relying on polymeric stabilizers or synthetic surfactants.

Accelerated storage at 40 °C confirmed the chemical and colloidal stability of the formulation, with <10 % vitamin D_3 loss after one month – consistent with ICH QINA-based predictive models consistent with a projected long-term shelf-life under ambient conditions.

4.3. Predicted bioavailability and mechanistic rationale

Although lipid-based nanocarriers are frequently investigated as strategies to enhance the oral delivery of hydrophobic bioactives (Viera Herrera et al., 2024; Zhang et al., 2022), direct demonstration of improved bioavailability requires dedicated biological and pharmacokinetic studies that fall outside the scope of the present work. The focus of this study is instead on the process–structure relationships governing the formation and physicochemical stability of nanoliposomal vitamin D_3. In this context, the Quality-by-Design analysis and the associated experimental investigation were aimed at clarifying how mixing conditions and formulation parameters influence key physicochemical attributes such as vesicle size, dispersion uniformity, and colloidal stability. These parameters are widely recognized as critical for the technological performance and manufacturability of lipid-based delivery systems, while their biological implications represent a logical direction for future investigation.

In particular, nanoscale vesicles with narrow size distributions and adequate colloidal stability are generally considered advantageous for dispersion in gastrointestinal fluids and for subsequent incorporation into mixed micelles during digestion.

Although in vivo pharmacokinetics were not evaluated, the physicochemical profile obtained here – nanometric size, narrow PDI, and near-neutral viscosity – is generally considered favorable for dispersion in gastrointestinal fluids and for subsequent incorporation into mixed micelles during digestion (Dymek and Sikora, 2022). This work focuses on technological performance; biological advantages remain to be investigated in future studies.

Experimental data from Dałek et al. (2022) showed that 120 nm vitamin D_3 liposomes yielded 2–3 × higher plasma 25(OH)D concentrations in rats than coarse emulsions, while Żurek et al. (2023) modeled size-dependent diffusion showing near-complete absorption below 200 nm. Smaller liposomes penetrate the mucus layer more efficiently (Andar et al., 2014; Latrobdiba et al., 2023) and can fuse with enterocyte membranes or release contents into mixed micelles.

Therefore, the sub-100 nm monodisperse liposomes obtained here are expected to exhibit superior oral bioaccessibility, while the additive-lean aqueous matrix enhances compliance and dosing accuracy.

4.4. Comparative advantages and sustainability aspects

The benchmarking study against five commercial products (Appendix A) revealed that marketed “liposomal” supplements are typically micron-sized, viscous, and compositionally complex, relying on glycerol, polysorbates, or gums to achieve apparent stability. In contrast, the proposed formulation achieves true nanoscale liposomes using only natural phospholipids and food-grade antioxidants.

From a green-chemistry perspective, the process operates at ambient temperature, uses ethanol as a recyclable solvent, and produces minimal waste – meeting several principles of sustainable manufacturing. Continuous coaxial-jet processing also has an energy demand substantially lower than typical sonication/homogenization processes.

Overall, the formulation combines nanoscale dispersion, low viscosity, and reduced excipient load, characteristics that may be advantageous for both technological performance and sustainable manufacturing.

4.5. Broader implications

By integrating chemical-engineering optimization (via Design of Experiments) with minimalist formulation design, this work exemplifies a Quality-by-Design (QbD) approach suitable for translational manufacturing. The established design space can serve as a template for other lipid-based pharmaceuticals, enabling predictive control over critical quality attributes (CQAs) such as size, PDI, and encapsulation efficiency.

Ultimately, this strategy bridges the gap between academic nanoparticle science and industrial production, supporting a new generation of sustainable, high-performance oral supplements.

5. Conclusions

This work demonstrates a robust, additive-lean, and scalable process for producing an aqueous nanoliposomal vitamin D_3 using a coaxial-jet mixing approach.

A three-factor Box–Behnken optimization on the drug-free phosphatidylcholine / ethanol / water system identified solvent flow rate and lipid concentration as the principal determinants of liposome size and ζ-potential, yielding a reproducible design space that remained valid when vitamin D_3 was incorporated.

The resulting dispersion featured sub-100 nm monomodal liposomes

(PDI ≈ 0.17, ζ ≈ –48 mV), encapsulation efficiency ≈ 99 %, and water-like viscosity (~3.7 cP), ensuring both physical stability and consumer acceptability.

Compared with five commercial "liposomal" references, the optimized product showed a particle size significantly smaller (sub-100 nm vs 0.2–1.6 μm), tighter PSD, quantitative label accuracy, and lower excipient load, all achieved in the same formulation.

The mild, solvent-efficient process satisfies several principles of green chemistry and aligns with the EU's circular-bioeconomy objectives.

Overall, the integration of process engineering and formulation design within a Quality-by-Design framework provides a structured approach for developing lipid-based formulations with controlled physicochemical properties.

The methodology is readily extendable to other hydrophobic bioactives, marking a step toward more sustainable and scientifically standardized supplement manufacturing.

CRediT authorship contribution statement

Diego Caccavo: Writing – review & editing, Validation, Supervision, Methodology, Investigation, Data curation. **Luca Broegg:** Writing – review & editing, Methodology, Investigation, Data curation. **Gaetano Lamberti:** Writing – original draft, Supervision, Conceptualization. **Raffaella De Piano:** Writing – review & editing, Methodology, Investigation, Conceptualization. **Anna Angela Barba:** Writing – review & editing, Supervision, Resources, Conceptualization.

Declaration of competing interest

The authors declare that they have no known competing financial interests or personal relationships that could have appeared to influence the work reported in this paper.

Appendix A

Comparative Performance vs. Commercial References.

The comparison reported in this appendix is intended solely as an exploratory technological benchmark aimed at contextualizing the physicochemical properties of the proposed formulation relative to commercially available aqueous vitamin D_3 products.

To do this, i.e. to benchmark the technological value of the optimized formulation, we compared it with five commercially available aqueous "liposomal" vitamin D_3 products. Products were anonymized (A–E) and purchased in European retail channels within expiration date. Comparisons must be considered as indicative rather than regulatory. The comparison with marketed formulations was therefore conducted strictly as a technological benchmark, with anonymized samples and standardized analytical conditions, to situate the performance of the proposed system within a realistic reference frame.

All samples were analyzed under identical experimental conditions using the same DLS, laser diffraction, rheological and HPLC protocols. The quantitative comparison is summarized in Table 4, combining four metrics – Z-average, being an indicator of nanoscale dispersion quality, which is a relevant physicochemical attribute for lipid-based oral delivery systems, was considered as a proxy for bioavailability (score Sc1), ζ-potential as a proxy for stability (Sc2), viscosity as a proxy for palatability (Sc3), the ratio between D_3 concentration measured, C_M, over the concentration declared, C_D, as a proxy for reliability (Sc4), while representative particle-size distributions are reported in Fig. 6. Each proxy has been assessed by a numerical score ranging from 0 (bad) to 5 (good).

Table 4
Comparative physicochemical characteristics of five commercial aqueous "liposomal" vitamin D3 products (A–E) and the optimized formulation developed in this study. Four measurable attributes were considered: Z-average diameter, ζ-potential, apparent viscosity, and the ratio between measured and declared vitamin D3 concentration (C_M/C_D). To facilitate qualitative comparison, each parameter was associated with a normalized score ranging from 0 (least favorable) to 5 (most favorable). The scores represent proxies for key technological attributes: particle size as an indicator of dispersion quality (Sc1), ζ-potential as an indicator of colloidal stability (Sc2), viscosity as an indicator of pourability/palatability (Sc3), and label accuracy (C_M/C_D) as an indicator of compositional reliability (Sc4). The overall score is obtained by summing the four individual scores.

	Z-average nm	Sc1	ζ-potential mV	Sc2	Viscosity cP	Sc3	D3 content C_M/C_D	Sc4	Overall /20
A	1602	1	−38.3	4	61	3	0.65	2	10
B	549	3	−26.0	3	13	4	0.65	2	12
C	701	2	−44.7	5	4060	1	0.41	1	9
D	245	4	−21.1	3	4.0	5	1.02	5	17
E	463	3	−8.73	1	4.0	5	1.56	4	13
This work	83	5	−48.3	5	3.7	5	1.00	5	20

The normalized comparison reported in Table 4 yielded an overall score of 20 / 20 for the optimized system versus an average of (12.2 ± 3.1)/20 for market references.

From a dimensional standpoint, the optimized formulation yielded a Z-average of 83 nm, whereas the marketed references ranged from 245 nm to 1.6 μm.

Laser-diffraction profiles (Fig. 6), which directly measure volume-based particle-size distributions, confirmed the presence of broad, polymodal distributions in the commercial samples, with substantial fractions in the micron range, suggestive of vesicle aggregation or incomplete micromixing during production. In contrast, the present formulation displayed a sharp monomodal peak centered at ~83 nm, consistent with the narrow PDI observed by DLS. Since nanoscale vesicles are more readily dispersed, more resistant to sedimentation, and more likely to interact favorably with intestinal colloidal structures, the Z-average was scored as a proxy for bioavailability (Sc1).

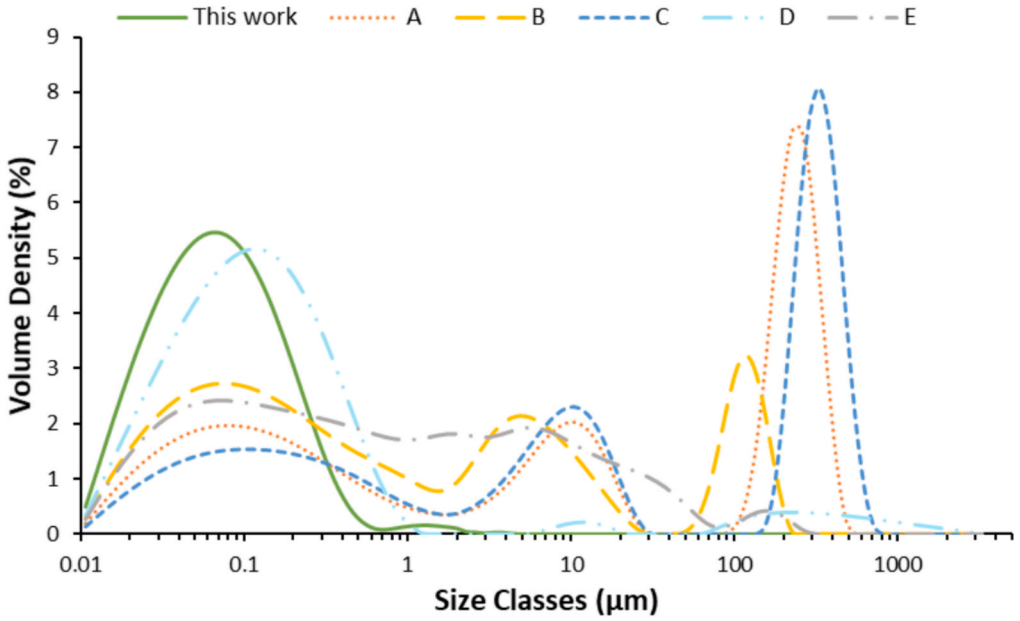

Fig. 6. Particle-size distributions of five commercial aqueous "liposomal" vitamin D_3 products (A–E) compared with the optimized nanoliposomal formulation developed in this work. Measurements were performed by laser diffraction, which directly provides volume-based particle-size distributions. Therefore, unlike the DLS measurements reported in Fig. 2, the volumetric PSD shown here represents the primary experimental output of the technique rather than a post-processed transformation of intensity data.

Electrostatic stability was evaluated through ζ-potential. Commercial products exhibited values between –8.7 and –44.7 mV, often near the empirical threshold for aggregation. The optimized formulation reached –48 mV, indicating strong electrostatic repulsion and reduced propensity for flocculation. This parameter was therefore used as a proxy for colloidal stability (Sc2). The combination of small size and highly negative ζ-potential suggests that the vesicles formed under coaxial-jet conditions are structurally uniform and kinetically stable.

Rheological behavior provided complementary information on user acceptability. Several commercial samples displayed viscosities ranging from 13 cP up to 4060 cP, values compatible with the presence of thickening agents or high dispersed-phase volume fractions. Such systems may improve apparent stability but compromise palatability, dosing precision, and perceived quality. By contrast, the optimized formulation showed a viscosity of 3.7 cP, essentially water-like, which was scored as a proxy for palatability (Sc3). Importantly, this low viscosity was achieved without sacrificing stability, owing to the nanoscale structure and appropriate surface charge.

Finally, the accuracy of vitamin D_3 content was assessed as the ratio between measured concentration (C_M) and declared concentration (C_D). Four out of five market references deviated substantially from label claims ($C_M/C_D = 0.41–0.65$), whereas the optimized product showed $C_M/C_D \approx 1.00$, both at baseline and after accelerated storage. This ratio was taken as a proxy for reliability (Sc4), integrating formulation robustness and manufacturing quality control.

When the four metrics were normalized and summed (Table 4), the optimized formulation achieved the maximum score (20/20), whereas commercial references averaged $(12.2 \pm 3.1)/20$. Product D performed comparatively better than the other references, mainly due to smaller mean size and accurate label content, but still lacked the combination of nanoscale dispersion, strong electrostatic stabilization, and favorable viscosity that characterizes the present system.

Overall, the comparative analysis demonstrates that the coaxial-jet–prepared formulation offers a unique balance of structural uniformity, physical stability, palatability, and dose reliability, achieved with a lean excipient profile. These attributes collectively explain how it outperforms commercially available aqueous "liposomal" vitamin D_3 suspensions, under the evaluated technological metrics.

Appendix B. Supplementary data

Supplementary data to this article can be found online at https://doi.org/10.1016/j.ijpharm.2026.126825.

Data availability

Data will be made available on request.

References

Adami, G., Fassio, A., 2021. Vitamin D supplementation: better daily or by bolus? Vitamin D - Update 4, 8–10. https://doi.org/10.30455/2611-2876-2021-2e.

Akar, S., Fardindoost, S., Hoorfar, M., 2024. High throughput microfluidics-based synthesis of PEGylated liposomes for precise size control and efficient drug encapsulation. Colloids Surf. B Biointerfaces 238, 113926. https://doi.org/10.1016/j.colsurfb.2024.113926.

Amjadi, S., Almasi, H., Hamishehkar, H., Kashaninejad, M., Ehsani, A., Jalili, S., 2024. Development of vitamin D3 and Spirulina platensis protein hydrolysates co-loaded nanoliposomes and coated by sodium caseinate. Food Struct. 42, 100399. https://doi.org/10.1016/j.foostr.2024.100399.

Andar, A.U., Hood, R.R., Vreeland, W.N., DeVoe, D.L., Swaan, P.W., 2014. Microfluidic preparation of liposomes to determine particle size influence on cellular uptake mechanisms. Pharm. Res. 31, 401–413. https://doi.org/10.1007/s11095-013-1171-8.

Barba, A.A., Lamberti, G., Bochicchio, S., 2017. Phenomenological and formulation aspects in tailored nanoliposome production. In: Catala, A. (Ed.), Liposomes. IntechOpen, London.

Bochicchio, S., Barba, A.A., Grassi, G., Lamberti, G., 2016a. Vitamin delivery: carriers based on nanoliposomes produced via ultrasonic irradiation. LWT Food Sci. Technol. 69, 9–16. https://doi.org/10.1016/j.lwt.2016.01.025.

Bochicchio, S., Dalmoro, A., Barba, A.A., d'Amore, M., Lamberti, G., 2017. New preparative approaches for micro and nano drug delivery carriers. Curr. Drug Deliv. 14, 203–215. https://doi.org/10.2174/1567201813666160628093724.

Bochicchio, S., Dalmoro, A., De Simone, V., Bertoncin, P., Lamberti, G., Barba, A.A., 2020a. Simil-microfluidic nanotechnology in manufacturing of liposomes as hydrophobic antioxidants skin release systems. Cosmetics 7, 22. https://doi.org/10.3390/cosmetics7020022.

Bochicchio, S., Dalmoro, A., Lamberti, G., Barba, A.A., 2020b. Advances in nanoliposomes production for ferrous sulfate delivery. Pharmaceutics 12, 445. https://doi.org/10.3390/pharmaceutics12050445.

Bochicchio, S., Dalmoro, A., Recupido, F., Lamberti, G., Barba, A.A., 2018. Nanoliposomes Production by a Protocol Based on a Simil-Microfluidic Approach, in: Piotto, S., Rossi, F., Concilio, S., Reverchon, E., Cattaneo, G. (Eds.), Advances in Bionanomaterials: Selected Papers from the 2nd Workshop in Bionanomaterials, BIONAM 2016, October 4-7, 2016, Salerno, Italy. Springer International Publishing, Cham, pp. 3-10.

Bondu, C., Yen, F.T., 2022. Nanoliposomes, from food industry to nutraceuticals: interests and uses. Innovative Food Sci. Emerg. Technol. 81, 103140. https://doi.org/10.1016/j.ifset.2022.103140.

Buttitta, G., Bonacorsi, S., Barbarito, C., Moliterno, M., Pompei, S., Saito, G., Oddone, I., Verdone, G., Secci, D., Raimondi, S., 2024. Scalable microfluidic method for tunable liposomal production by a design of experiment approach. Int. J. Pharm. 662, 124460. https://doi.org/10.1016/j.ijpharm.2024.124460.

Caccavo, D., De Piano, R., Broegg, L., Barba, A.A., Lamberti, G., 2025. Optimization of nanoliposomes production using a coaxial jet mixer: a response surface modeling approach. Chem. Eng. Trans. 118, 295–300. https://doi.org/10.3303/CET25118050.

Caccavo, D., Lamberti, G., Barba, A.A., 2023. Coaxial injection mixer for the continuous production of nanoparticles. Chem. Eng. Trans. 100, 301–306. https://doi.org/10.3303/CET23100051.

Cashman, K.D., Dowling, K.G., Škrabáková, Z., Gonzalez-Gross, M., Valtueña, J., De Henauw, S., Moreno, L., Damsgaard, C.T., Michaelsen, K.F., Mølgaard, C., Jorde, R., Grimnes, G., Moschonis, G., Mavrogianni, C., Manios, Y., Thamm, M., Mensink, G.B. M., Rabenberg, M., Busch, M.A., Cox, L., Meadows, S., Goldberg, G., Prentice, A., Dekker, J.M., Nijpels, G., Pilz, S., Swart, K.M., van Schoor, N.M., Lips, P., Eiriksdottir, G., Gudnason, V., Cotch, M.F., Koskinen, S., Lamberg-Allardt, C., Durazo-Arvizu, R.A., Sempos, C.T., Kiely, M., 2016. Vitamin D deficiency in Europe: pandemic? Am. J. Clin. Nutr. 103, 1033–1044. https://doi.org/10.3945/ajcn.115.120873.

Chaves, M.A., Dacanal, G.C., Pinho, S.C., 2023a. High-shear wet agglomeration process for enriching cornstarch with curcumin and vitamin D3 co-loaded lyophilized liposomes. Food Res. Int. 169, 112809. https://doi.org/10.1016/j.foodres.2023.112809.

Chaves, M.A., Ferreira, L.S., Baldino, L., Pinho, S.C., Reverchon, E., 2023b. Current applications of liposomes for the delivery of vitamins: a systematic review. Nanomaterials 13, 1557. https://doi.org/10.3390/nano13091557.

Dałek, P., Drabik, D., Wołczańska, H., Foryś, A., Jagas, M., Jędruchniewicz, N., Przybyło, M., Witkiewicz, W., Langner, M., 2022. Bioavailability by design — vitamin D3 liposomal delivery vehicles. Nanomed. Nanotechnol. Biol. Med. 43, 102552. https://doi.org/10.1016/j.nano.2022.102552.

Dalmoro, A., Bochicchio, S., Lamberti, G., Bertoncin, P., Janssens, B., Barba, A.A., 2019. Micronutrients encapsulation in enhanced nanoliposomal carriers by a novel preparative technology. RSC Adv. 9, 19800–19812. https://doi.org/10.1039/C9RA03022K.

Dymek, M., Sikora, E., 2022. Liposomes as biocompatible and smart delivery systems – the current state. Adv. Colloid Interface Sci. 309, 102757. https://doi.org/10.1016/j.cis.2022.102757.

Fan, C., Feng, T., Wang, X., Xia, S., John Swing, C., 2023. Liposomes for encapsulation of liposoluble vitamins (a, D, E and K): comparation of loading ability, storage stability and bilayer dynamics. Food Res. Int. 163, 112264. https://doi.org/10.1016/j.foodres.2022.112264.

Grand View Research, 2024a. Dietary Supplements Market (2025 - 2033) https://www.grandviewresearch.com/industry-analysis/dietary-supplements-market-report, Accessed: 21/11/2025.

Grand View Research, 2024b. Nutraceuticals Market (2025 - 2030) https://www.grandviewresearch.com/industry-analysis/nutraceuticals-market, Accessed: 21/11/2025.

Guimarães, D., Cavaco-Paulo, A., Nogueira, E., 2021. Design of liposomes as drug delivery system for therapeutic applications. Int. J. Pharm. 601, 120571. https://doi.org/10.1016/j.ijpharm.2021.120571.

Iannone, M., Caccavo, D., Barba, A.A., Lamberti, G., 2022. A low-cost push–pull syringe pump for continuous flow applications. HardwareX 11, e00295. https://doi.org/10.1016/j.ohx.2022.e00295.

ICH Q1A, R., 2003. ICH Q1A (R2) Stability testing of new drug substances and drug products - Scientific guideline.

Lamberti, G., Barba, A.A., Caccavo, D., Broegg, L., 2025, Formulazione di un integratore alimentare di vitamina D3 liposomiale, IT102025000035608.

Latrobdiba, Z.M., Fulyani, F., Anjani, G., 2023. Liposome optimisation for oral delivery of nutraceuticals in food: a review. Food Res. 7, 233–246. https://doi.org/10.26656/fr.2017.7(3).022.

Lim, J.-M., Swami, A., Gilson, L.M., Chopra, S., Choi, S., Wu, J., Langer, R., Karnik, R., Farokhzad, O.C., 2014. Ultra-high throughput synthesis of nanoparticles with homogeneous size distribution using a coaxial turbulent jet mixer. ACS Nano 8, 6056–6065. https://doi.org/10.1021/nn501371n.

Lim, S.W.Z., Wong, Y.S., Czarny, B., Venkatraman, S., 2020. Microfluidic-directed self-assembly of liposomes: role of interdigitation. J. Colloid Interface Sci. 578, 47–57. https://doi.org/10.1016/j.jcis.2020.05.114.

Lindsay, S., Tumolva, O., Khamiakova, T., Coppenolle, H., Kovarik, M., Shah, S., Holm, R., Perrie, Y., 2024. Can we simplify liposome manufacturing using a complex DoE approach? Pharmaceutics 16, 1159. https://doi.org/10.3390/pharmaceutics16091159.

Makino, Y., Matugi, H., Suzuki, Y., 1993, Stabilized aqueous preparation of active form of vitamin D3, US 5182274 A.

Market.us, 2025. Global Vitamin D3 Market Size, Share, And Business Benefits, https://market.us/report/vitamin-d3-market/, Accessed: 21/11/2025.

Mazess, R.B., Bischoff Ferrari, H.A., Dawson Hughes, B., 2021. Vitamin D: bolus is bogus—a narrative review. JBMR Plus 5, e10567. https://doi.org/10.1002/jbm4.10567.

Mehraji, S., DeVoe, D.L., 2024. Microfluidic synthesis of lipid-based nanoparticles for drug delivery: recent advances and opportunities. Lab Chip 24, 1154–1174. https://doi.org/10.1039/D3LC00821E.

Mordor Intelligence, 2025. Vitamin D Supplement Market Size & Share Analysis - Growth Trends And Forecast (2025 - 2030), https://www.mordorintelligence.com/industry-reports/vitamin-d-supplements-market, Accessed: 21/11/2025.

Musakhanian, J., Rodier, J.-D., Dave, M., 2022. Oxidative stability in lipid formulations: a review of the mechanisms, drivers, and inhibitors of oxidation. AAPS PharmSciTech 23, 151. https://doi.org/10.1208/s12249-022-02282-0.

Pasarin, D., Ghizdareanu, A.-I., Enascuta, C.E., Matei, C.B., Bilbie, C., Paraschiv-Palada, L., Veres, P.-A., 2023. Coating materials to increase the stability of liposomes. Polymers 15, 782. https://doi.org/10.3390/polym15030782.

Patterson, G.K., Paul, E.L., Kresta, S.M., Etchells Iii, A.W., 2003. Mixing and chemical reactions. Handbook of Industrial Mixing 755–867.

Penoy, N., Delma, K.L., Homkar, N., Karim Sakira, A., Egrek, S., Sacheli, R., Sacré, P.-Y., Grignard, B., Hayette, M.-P., Somé, T.I., Semdé, R., Evrard, B., Piel, G., 2024. Development and optimization of a one step process for the production and sterilization of liposomes using supercritical CO2. Int. J. Pharm. 651, 123769. https://doi.org/10.1016/j.ijpharm.2024.123769.

Pittiu, A., Pannuzzo, M., Casula, L., Pireddu, R., Valenti, D., Cardia, M.C., Lai, F., Rosa, A., Sinico, C., Schlich, M., 2024. Production of liposomes by microfluidics: the impact of post-manufacturing dilution on drug encapsulation and lipid loss. Int. J. Pharm. 664, 124641. https://doi.org/10.1016/j.ijpharm.2024.124641.

Pouton, C.W., Porter, C.J.H., 2008. Formulation of lipid-based delivery systems for oral administration: materials, methods and strategies. Adv. Drug Deliv. Rev. 60, 625–637. https://doi.org/10.1016/j.addr.2007.10.010.

Rudzińska, M., Grygier, A., Knight, G., Kmiecik, D., 2024. Liposomes as carriers of bioactive compounds in human nutrition. Foods 13, 1814. https://doi.org/10.3390/foods13121814.

Saad, W.S., Prud'homme, R.K., 2016. Principles of nanoparticle formation by flash nanoprecipitation. Nano Today 11, 212–227. https://doi.org/10.1016/j.nantod.2016.04.006.

Sainaga Jyothi, V.G.S., Bulusu, R., Venkata Krishna Rao, B., Pranothi, M., Banda, S., Kumar Bolla, P., Kommineni, N., 2022. Stability characterization for pharmaceutical liposome product development with focus on regulatory considerations: an update. Int. J. Pharm. 624, 122022. https://doi.org/10.1016/j.ijpharm.2022.122022.

Sameer Khan, M., Gupta, G., Alsayari, A., Wahab, S., Sahebkar, A., Kesharwani, P., 2024. Advancements in liposomal formulations: a comprehensive exploration of industrial production techniques. Int. J. Pharm. 658, 124212. https://doi.org/10.1016/j.ijpharm.2024.124212.

Spherical Insights, 2024. Global Vitamin D Market Size, Share, and COVID-19 Impact Analysis, https://www.sphericalinsights.com/reports/vitamin-d-market, Accessed: 21/11/2025.

Temova Rakuša, Ž., Pišlar, M., Kristl, A., Roškar, R., 2021. Comprehensive stability study of vitamin D3 in aqueous solutions and liquid commercial products. Pharmaceutics 13, 617. https://doi.org/10.3390/pharmaceutics13050617.

Tripkovic, L., Lambert, H., Hart, K., Smith, C.P., Bucca, G., Penson, S., Chope, G., Hyppönen, E., Berry, J., Vieth, R., Lanham-New, S., 2012. Comparison of vitamin D2 and vitamin D3 supplementation in raising serum 25-hydroxyvitamin D status: a systematic review and meta-analysis123. Am. J. Clin. Nutr. 95, 1357–1364. https://doi.org/10.3945/ajcn.111.031070.

Viera Herrera, C., O'Connor, P.M., Ratrey, P., Paul Ross, R., Hill, C., Hudson, S.P., 2024. Anionic liposome formulation for oral delivery of thuricin CD, a potential antimicrobial peptide therapeutic. Int. J. Pharm. 654, 123918. https://doi.org/10.1016/j.ijpharm.2024.123918.

Yi, X., Gao, S., Gao, X., Zhang, X., Xia, G., Liu, Z., Shi, H., Shen, X., 2023. Glycolipids improve the stability of liposomes: the perspective of bilayer membrane structure. Food Chem. 412, 135517. https://doi.org/10.1016/j.foodchem.2023.135517.

Zhang, R., Zhang, Q., Oliveira, H., Mateus, N., Ye, S., Jiang, S., He, J., Wu, M., 2022. Preparation of nanoliposomes loaded with anthocyanins from grape skin extracts: stability, gastric absorption and antiproliferative properties. Food Funct. 13, 10912–10922. https://doi.org/10.1039/D2FO02008D.

Żurek, G., Przybyło, M., Witkiewicz, W., Langner, M., 2023. Novel approach for the approximation of vitamin D3 pharmacokinetics from in vivo absorption studies. Pharmaceutics 15, 783. https://doi.org/10.3390/pharmaceutics15030783.